8-1-2019

Dynamics of liposomes in the fluid phase

Sudipta Gupta
Louisiana State University

Judith U. De Mel
Louisiana State University

Gerald J. Schneider
Louisiana State University

Recommended Citation

Gupta, S., De Mel, J., & Schneider, G. (2019). Dynamics of liposomes in the fluid phase. *Current Opinion in Colloid and Interface Science, 42*, 121-136. https://doi.org/10.1016/j.cocis.2019.05.003

Dynamics of Liposomes in the Fluid Phase

Sudipta Gupta,[1] Judith U. De Mel,[1] Gerald J. Schneider[1,2]

[1]*Department of Chemistry, Louisiana State University, Baton Rouge, LA 70803, USA*

[2]*Department of Physics & Astronomy, Louisiana State University, Baton Rouge, LA 70803, USA*

1. Abbreviations

1,2-dimyristoyl-sn-glycero-3-phosphocholine (DMPC); 1,2-distearoyl-sn-glycero-3-phosphocholine (DSPC); 1,2-dipalmitoyl-sn-glycero-phosphocholine (DPPC); 1,2-dioleoyl-sn-glycero-phosphocholine (DOPC); 1-palmitoyl-2-oleoyl-glycero-3-phosphocholine (POPC); L-α-Phosphatidylcholine (SoyPC); egg lecithin (EYPC); dimyristoylphosphatidyl-ethanolamine (DMPE); galactosyl-diacylglycerol (G-DG); digalactosyl-diacylglycerol (DGDG); 1-stearoyl-2-oleoyl-sn-glycero-3-phosphocholine (SOPC); diarachidonyl phosphatidyl-choline (DAPC); 1,2-diheptanoyl-sn-glycero-3-phosphocholine (DHPC); 1,2-dilinoleoyl-sn-glycero-3-phosphocholine (DLPC); 1-palmitoyl-2-oleoylphosphatidic acid (POPA); poly(ethylene glycol) (PEG); nanoparticles (NPs); phosphatidylserine (PS); phosphatidylglycerol (PG); phosphatidylethanolamine (PE); phosphatidylcholine (PC); 1,2 –dimyristoyl –sn-glycero-3-phosphoglycerol (DMPG); Electron Spin Resonance (ESR); sodium dodecylsulphate (SDS); 4-(2-hydroxyethyl)-1-piperazineethanesulfonic acid (HEPES); 2-(N-morpholino) ethanesulfonic acid (MES); 3-(N morpholino) propanesulfonic acid (MOPS); piperazine-N , N′ -Bis (2-ethanesulfonic acid) (PIPES); tris(hydroxymethyl)-aminomethane (TRIS), ethylene-diamine-tetraacetic acid (EDTA); specific gravity from density meter (SG); Differential Scanning Calorimetry (DSC)

2. Abstract

We review the currently available material on the morphology and dynamics of phospholipids assembled into liposomes. Key information obtained from neutron scattering, NMR, and other techniques plays a crucial role to understand the vital role of lipids in sustaining life in living organisms. We concentrate on the dynamics in the biologically important fluid phase in the time

range from picoseconds to seconds, which includes a discussion of the center of mass diffusion of liposomes, membrane fluctuations, lateral, rotational and flip-flop motions of the lipids. We emphasize on the sensitivity of the dynamics on interactions with a variety of biologically relevant molecules such as cholesterol. By a comparison of data from literature, we witness a good agreement of the results from different techniques and studies.

3. Introduction

Liposomes are spherical vesicles that encapsulate an aqueous core by a bilayer formed by amphiphilic phospholipids. Phospholipids constitute the major part of the cell membrane. The physical properties of cell membrane are optimized for both cellular barrier as well as selective gateways. It protects the interior of the cell membranes from a potential hostile environment. Lipid membranes are model systems of a two-dimensional surfaces in three-dimensional space and allow us to study them at molecular and atomic level. They exhibit unique viscoelastic properties essential for the biological functioning of the living cell. It's a grand challenge to understand the fundamentals of self-organization of such a multi-component system that leads to complex interactions, structures, and dynamics. For example the role of a lipid bilayer undergoing spontaneous curving, bending as observed in large unilamellar vesicles, that leads to the formation of multilamellar vesicles, vesicle budding, vesicle fusion and synaptic vesicle exocytosis, is still not well understood [1]. Lipids contribute to cell division [2] and reproduction [3] but the corresponding physical principles and methodologies are still not solved. Much overlooked dynamics such as lipid rotation have shown to be affected by hydrostatic pressure, lipid phase and additives such as cholesterol content [4, 5]. Lipid flip-flop motion is another dynamic process which occurs in relatively larger time scales. It is crucial for maintaining lipid composition in the inner and outer monolayers of the membrane [6]. All of these processes form the basis to understand the evolution of life. On the other hand, the importance of vesicles and membranes in biotechnical application is unchallenged, like, vesicles used for drug delivery cargo [7], or integration of membranes with electronic/optoelectronic devices to build biosensors [8].

This review concentrates on the dynamics in the biologically very important fluid phase, often more accurately referred to as liquid crystalline phase, L_α. It is separated from the gel phase, ($L_{\beta'}$) by a certain melting transition temperature, T_m. In the fluid phase the hydrocarbon chains of the lipid tails are liquid like, disordered and randomly oriented [9]. The lipid membrane has a unique molecular structure that resembles both liquid-like viscous component and elastic liquid-crystalline part [10]. The conformation of the lipid chain is related to the thermodynamics and to the mechanical properties of the membrane, like, bending rigidity and elasticity that defines the spontaneous curvature of the bilayer [9, 11]. Hereafter we concentrate on spherical liposomes on a length-scale of the order of 50 to 200 nm. Often the literature distinguishes large unilamellar vesicles (LUVs, 50 to 200 nm) and giant unilamellar vesicles (GUVs, diameters on the order 1 to 10 µm). As illustrated in figure 1, the variability of these so-called liposomes results from the lipid flexibility, including head group chemistry, hydrocarbon chain lengths of the fatty acids and their level of unsaturation. Its combination determines many properties, like T_m [11-13].

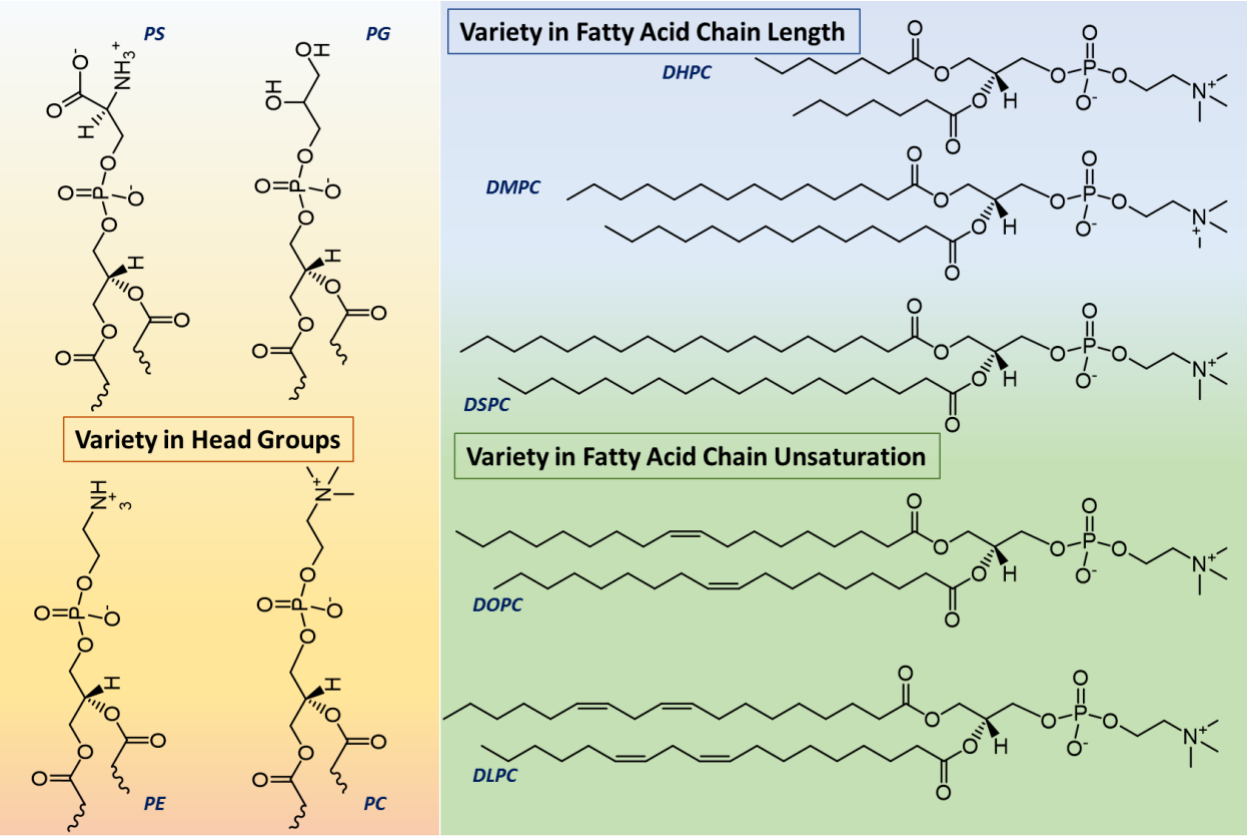

Figure 1: Schematic drawing of phospholipids and phospholipid head groups.

4. Morphology of vesicles

The morphology of liposomes is defined by the bending elasticity of the lipid bilayer [9]. Based on the spontaneous curvature model introduced by Helfrich [12] the curvature energy, F_{sc}, of a closed 2D surface is given by

$$F_{sc} = \frac{\kappa}{2}\oint dA\ (2H - C_0)^2 + \kappa_G \oint dA \quad K \tag{1}$$

The mean curvature, $H = (1/R_1 + 1/R_2)/2$, and the Gaussian curvature, $K = 1/(R_1 R_2)$, can be deduced from the two radii, R_1 and R_2. The parameters, κ and κ_G, are the bending rigidity and Gaussian bending rigidity, respectively. The spontaneous curvature, C_0, defines the asymmetry of the shape fluctuations, and is assumed to depend on the environment chemistry and the bilayer architecture [9].

Seifert *et al.* proposed the formation of bowl (tomatocytes), oblate, prolate, and pear shaped vesicles by changing different parameters like the reduced volume, $v = V/V_0$, C_0, or temperature, T [13]. Domain induced budding was proposed by Jülicher *et al.* [14], whereas lateral phase separation was introduced by Seifert [15]. These objects have been discovered experimentally by phase contrast microscopy [16-18]. Hereafter, we focus on the spherical structures.

Detailed information on the structure of liposomes and membranes has been obtained by scattering techniques. Nagele *et al.* utilized X-ray diffraction to deduce information on the number of bilayers [19, 20]. Different theoretical approaches exist to describe the structure factor of multilamellar liposomes, e.g., by Frielinghaus [21]. More detailed information on the distribution of molecules in the bilayer itself has been obtained by a joint refinement of X-ray and neutron diffraction data [22]. This method determines a quasimolecular structure consisting of fragments representing the methylene regions by Gaussian distributions.

Our discussion implies that the lipids are aggregated to liposomes, i.e., the system itself is at (lipid) concentrations, Φ, greater than the critical micellar concentration (CMC) of the lipids, often also referred to as critical vesicular concentration (CVC) or critical aggregation concentration (CAC). Many different experimental approaches permit to determine the CMC

[23]. Mole fractions seem to be lesser than mM usually [24]. The textbook by Marsh provides a comprehensive overview and reports CMC values in the range of 10^{-9} to 10^{-3} M [24]. The experiments reviewed below used conditions $\Phi >> CMC$. Hence, we neglect the contribution of the free lipids to the experimental results in our discussion.

5. Dynamics of Liposomes at Different Length- and Time-Scales

As figure 2 illustrates, many different processes are anticipated in liposomes, even if a spherically symmetric morphology is assumed. Individual molecular motions and their collective dynamics capture a broad range of length- and time scales and may even be viewed in terms of hierarchical structures and dynamics. Lipid membrane motions can vary from picoseconds to several hours spanning many decades of the time scale as shown in figure 2 [25]. Therefore, using multiple techniques becomes a vital part in unveiling membrane dynamic processes. In the subsequent sections we will discuss these motions in detail.

For the sake of simplicity, we have omitted vesicle fusion from our discussion. As will be detailed later and illustrated in figure 2, translational diffusion of liposomes refers to the Brownian diffusion of the center of mass of liposomes in the respective solvent (section 6.2). Liposomes can be considered as flexible colloids. Section 5.2 reports experimental findings and discusses the relevance to the biological function. In view of the motions of the bilayer itself, several processes can be identified such as shape fluctuations [26], thickness fluctuations and membrane undulations. Membrane fluctuations represent collective motion of the bilayer that may lead to breathing mode (symmetric deformation), deformations modes (asymmetric deformation), undulations, etc. [11]. Membrane undulation includes fluctuation of the membrane in the 2D plane due to thermal noise. It is related to the membrane rigidity as discussed in section 5.2. On the other hand, the membrane thickness fluctuations represent individual motion of the leaflets that lead to thickness fluctuation perpendicular to the 2D plane [27, 28]. We explore theoretical and experimental details in section 5.3. At faster times additional lipid lateral [29] [30] and lipid rotational motion along its symmetry axis become visible (sections 6.5 and 6.6 respectively)[5]. In case of the so called “flip-flop” motions, the exchange of lipids across the bilayer occurs at much slower times as explained in section 6.7. Time scale of individual lipid dynamics does not have a direct proportionality to their size but rather depends on the process

and the length scale of focus. For instance, individual lipids also show vibrational motions which can be accessed by FT-IR methods at a time scale approx. 10^{-10} s while being able to flip-flop which may take up to several hours [31].

Length-scales of dynamic processes in liposomes are important in understanding the scope of dynamics and some must be expressed with respect to time. Membrane fluctuations such as undulations, thickness fluctuations occur typically at a mesoscopic length scale (10 to 1000 Å) [32] and lateral diffusion at micrometer scale [33]. Wanderling et.al have shown a slow diffusion of individual lipids in a confined cylindrical space in addition to the well-known conformational motions of the fatty acid chains and fast uniaxial rotations of H atoms around the C bonds. All of these dynamics occur in few Angstrom to a few nanometers length scale.[34] [35].

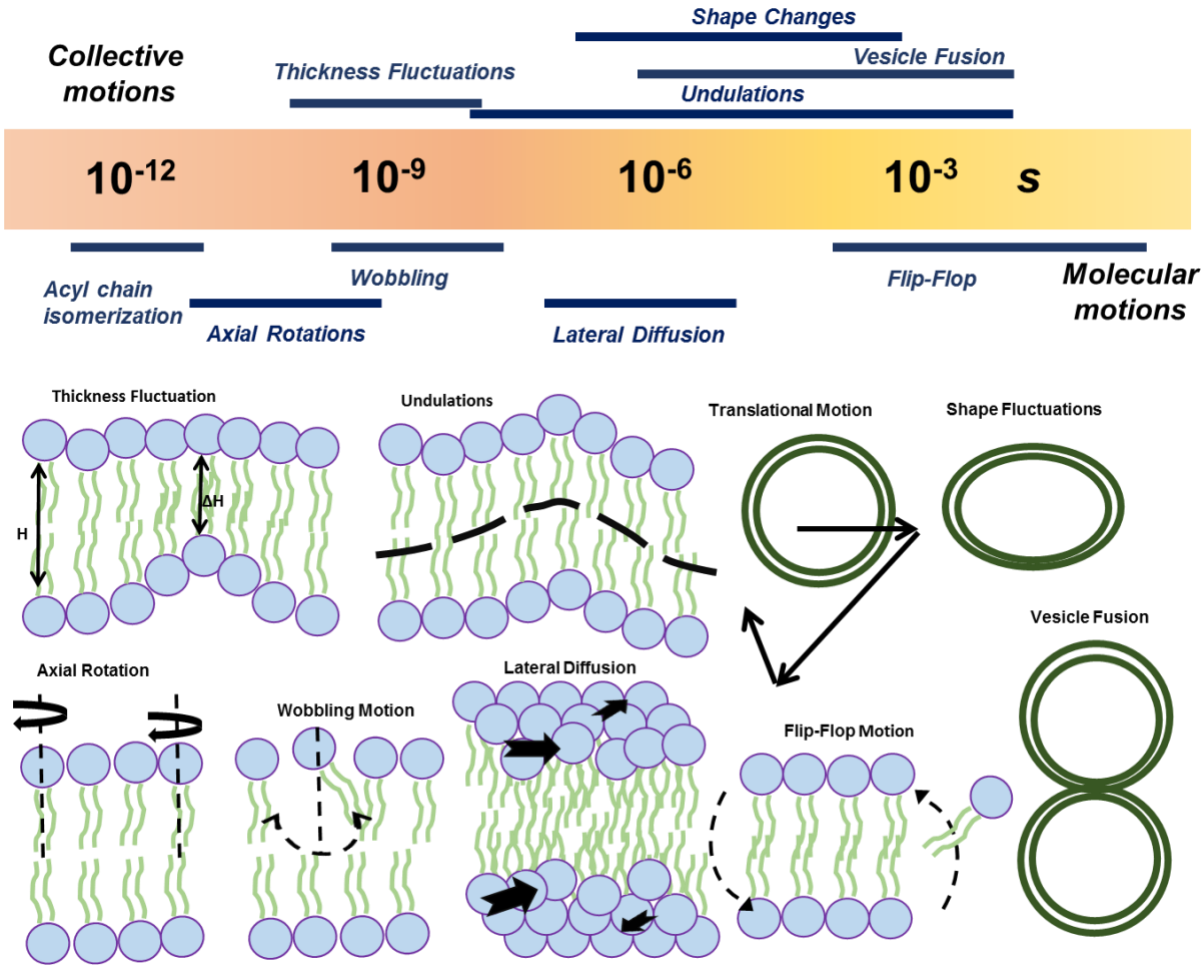

Figure 2: Different dynamics at different time scales. Acyl chain motions[35]Lateral diffusion[36]wobbling[37]

5.1. Liposome translational diffusion

Starting at the largest length-scale and the simplest structural case, liposomes can be considered as spherical colloidal particles that undergo Brownian motion in aqueous solution [11]. Dynamic light scattering is a technique commonly used to measure the translational diffusion coefficient, D_t. The Stokes-Einstein relation, $D_t = k_B T/(6\pi\eta_s R_h)$, connects D_t and the length-scale, represented by the hydrodynamic radius, R_h. The thermal fluctuations that cause the Brownian motion of the liposomes enter via the thermal energy, $k_B T$, with the Boltzmann constant, k_B, and the temperature, T (in K). The parameter, η_s refers to the viscosity of the solvent.

Depending on their preparation, the hydrodynamic radii of liposomes can vary from 20 nm to ~ 50 μm [38, 39]. From the Stokes-Einstein relation, we can estimate the associated range of translational diffusion coefficients from 1.2×10^{-11} to 5×10^{-15} m^2/s. ($R_h \approx 50$ nm then $D_t \approx 10^{-12}$ $m^2 s^{-1}$.) Beyond the case of an infinitely diluted system, colloidal interactions may become important. For example, Batchelor [40] and later Cichocki and Felderhof [41] calculated the long-time self-diffusion coefficient, D_S^L, of hard sphere colloids, $D_S^L = D_0(1 - 2.0972\phi)$, with, D_0, the diffusion coefficient at infinite dilution and, ϕ, the volume fraction of the colloids, not to be mixed up with the previously introduced concentration of lipids, Φ. The simple linear relationship shows that at a hypothetical liposome concentration of around 0.47 the self-diffusion would tend to be zero.

At the first glance, it seems to be simple to determine the diffusion coefficient, including the availability of a selection of tools to permit the correct numerical values. Often, certain limitations seem to require more effort than expected. For example, pulsed field gradient (PFG) NMR is a common technique to measure the self-diffusion coefficient of macromolecules. In case of micelles the self-diffusion measured by DLS and PFG-NMR usually agree [42]. However, in case of liposomes, Odeh *et al.* report a larger diffusion coefficient for the pure liposomes than one would expect from other techniques like DLS [43]. The authors explain the not-well defined signals of the PFG NMR experiment by the inherent rigidity of the bilayer and demonstrated the importance of adding a hydrotropic agent, like poly(ethylene glycol) (PEG), to obtain the true diffusion coefficient. In case of PEGylated liposomes Leal *et.al.* report $D_t =$

$5.2 \times 10^{-12}\ \mathrm{m}^2/s$, which corresponds to a size of 84 nm and to the values expected from DLS [44]. However, usually, colloidal science introduces a structure factor contribution to accomplish agreement, this these observations deserve further investigation.

5.2. Membrane Fluctuations (Undulations)

As illustrated by figure 2, membranes undergo out-of-plane fluctuations, often referred to as undulations, due to thermal excitations. The spectrum of fluctuation frequencies determines essentially the bending elasticity, κ_η, of the membrane. The value is characteristic for certain chemical compositions and morphologies and is seen as one of the most important physical parameters. It is related to the stability and shape of liposomes, the inter-liposome interactions, as well as interactions of the liposomes with foreign objects, like, drugs, nanoparticles, polymers, planar substrates, etc. [9]. It is also responsible for the phenomenon of polymorphism of the lipids that allow them to aggregate into different structures and phases, such as liquid crystalline phases under external perturbations like, changes in pH, temperature, pressure, volume, etc. [11].

The lipid membrane has the unique molecular structure that resembles both a liquid-like viscous component and the elastic liquid-crystalline part. The conformation of the lipid chain is related to the thermodynamic and mechanical properties of the membrane, like, bending rigidity and stretching elasticity that defines the spontaneous curvature of the bilayer, whereas, the shear modulus inside a fluid membrane is zero [9, 12, 45, 46]. The stretching elasticity accounts for the increase in the average distance between the molecules perpendicular to the bilayer neutral plane. The corresponding area compressibility modulus, K_A, is proportional the relative change in surface area, $\Delta A/A = \sigma/K_A$, for a given lateral stress, σ. Micromechanical analysis and X-ray diffraction reveal that the stretching of the lipid bilayer is limited to rather small deformations and rupture occurs even at a small change in area ($\Delta A/A \sim 1\%$) [47]. Therefore, lipid bilayers behave like a planar surface and can undergo a smooth shape deformation along the bilayer surface normal that depends on the bending rigidity, κ_η, of the lipid bilayer.

Neutron Spin Echo (NSE) spectroscopy has been frequently utilized to determine the bending rigidity, κ_η, of the lipid bilayer [10, 27, 28, 48-54]. NSE measures the time dependent structure

factor, $S(Q,t)$, as a function of the momentum transfer, Q. Assuming quasielastic scattering $Q = 4\pi/\lambda \sin(\vartheta)$, with the wave-length, λ, of the incident neutrons and the scattering angle, ϑ. The reciprocal relationship $Q = 2\pi/\ell$ connects the momentum transfer with the size or length-scale, ℓ, of the scattering objects in the sample. Measuring $S(Q,t)$ allows to distinguish different processes by their length- and time scale, which is essential for liposomes, e.g., to distinguish the slow translational diffusion of the liposomes from the faster motion of lipids. Individual NSE instruments can capture a time-range from 0.01 ns to 500 ns and a length-scale range of around 1-30 nm [55].

NSE has often been used to measure the dynamics of membranes. The common approach to extract information on the undulations utilizes a simplified theory for an ensemble of membrane patches following the Zilman-Granek (ZG) model [56]. It assumes the intermediate scattering function

$$\left(\frac{S(Q,t)}{S(Q)}\right)_{ZG} = \exp\left[-\left(\Gamma_Q t\right)^{2/3}\right] \tag{2}$$

is connected to a Q-dependent decay rate, Γ_Q, which depends on the intrinsic bending modulus, κ_η [10, 48, 57, 58]

$$\frac{\Gamma_q}{Q^3} = 0.0069\gamma\frac{k_BT}{\eta_s}\sqrt{\frac{k_BT}{\kappa_\eta}} \tag{3}$$

The term k_BT represents the thermal energy with the Boltzmann constant, k_B, and the temperature, T. The temperature dependent solvent viscosity, η_s, can be determined independently using a viscometer [59]. While there seems to be no rigorous theoretical proof, recent experiments seem to justify the established procedure of using η_s instead of the solution viscosity. Usually, $\kappa_\eta/k_BT \gg 1$ is assumed that leads to $\gamma \approx 1 - \frac{3}{4\pi}\frac{k_BT}{\kappa_\eta}\ln(Q\xi) \approx 1$, with the length-scale, ξ, of the fluctuations of the membrane [10, 27, 48, 56, 60].

Zilman and Granek first introduced a prefactor 0.025 (instead of 0.0069). Then 0.0058 was calculated assuming a ratio, $\delta/(2\delta_T) \approx 0.6$, between the distance of the neutral surface from the

bilayer midplane, δ, and the thickness of the monolayer, δ_T. However, this moves the neutral surface into the headgroup region of the bilayer, which turned out to be impossible. It finally led to the assumption that $\delta = \delta_T$ and which resulted in a numerical prefactor 0.0069 [10, 48]. Since different publications use different prefactors, the comparison of the bending moduli requires a recalculation. Therefore, table 1 summarizes the original values and calculates κ_η for the prefactor 0.0069, the most recent value. While the ZG model seems to be more appropriate for vesicles with a radius R ≥ 20 nm [61], in some cases the Milner-Safran seem to be more suitable for microemulsion droplets [62]. The relaxation spectrum according to ZG theory relaxes at a slower rate for rigid membranes as observed in phospholipids, in comparison to that observed in most microemulsions droplets and their sponge phases [63-65]. The faster relaxation of bending modes in microemulsions results in super flexible systems, with $\kappa_\eta/k_BT \lesssim 1$. In the fluid phase, κ_η was found to decrease linearly with temperature [10], increases dramatically with decrease in size [66], decreases with decrease in pH [67], and varies abruptly in presence of different additives, cf. table 1.

Equation 2 assumes ZG motion but neglects translational diffusion of liposomes. As defined by the diameter and the related diffusion coefficient, D_t, a substantial contribution to the intermediate structure factor within the typical time-window of NSE experiments can be expected [48]. We can incorporate the influence of diffusion in the dynamic structure factor by assuming that ZG and center of mass motion are statistically independent, which leads to a product ansatz [48, 68]

$$\frac{S(Q,t)}{S(Q)} = \exp(-D_t Q^2 t) \exp\left[-\left(\Gamma_q t\right)^{\frac{2}{3}}\right]. \qquad (4)$$

Though there is no rigorous theoretical proof that diffusion and ZG are statistically independent, this assumption permits to determine D_t independently from Γ_Q, either by analyzing the time and Q-dependence of $S(Q,t)$ or by complementary experiments, such as DLS [58].

For the fluid phases, L_α, of h-DOPC, h-DMPC, h-DPPC, h-DSPC, and h-POPC liposomes, values of $\kappa_\eta \approx 20\ k_BT$ are reported [27, 52, 53] [69]. (The exact values are listed in table 1). A much smaller value $\kappa_\eta = 8.4 \pm 1\ k_BT$ was observed for h-SoyPC [58]. Linear increases in

κ_η with decreasing temperature and approaching the transition temperatures are reported for dt-DMPC, dt-DPPC and dt-DSPC, all in L_α phase, by Nagao *et al*. [10].

Several experimental techniques can measure membrane fluctuations. Typical values seem to be on the order of $\kappa_\eta \approx$ 10-20 k_BT [70, 71]. Examples are flickering spectroscopy that used image processing methods and Fourier analysis to study thermally induced shape fluctuations on DMPC, EYPC, DMPE, G-DG and DGDG membranes in the fluid state [70, 71]. Another approach, like entropic tension micropipette includes aspiration of vesicles in a micropipette that changes the area available for mechanical fluctuations [47, 72, 73]. From the relation between the fluctuation area and suction pressure, thereby the effective entropic tension one can determine κ_η. Lipids like DGDG, DMPC, SOPC and DAPC were studied in the L_α phase. It should be noted that apart from, κ_η, the other two elastic parameters, K_A, and the corresponding thermal expansion coefficient, α_A, can be determined in general by aspiration pipet method [47, 73]. Mechanical fluctuations can also be implemented using electric deformation [74, 75].

Several studies indicate interactions of nanoobjects with liposomes impact the membrane rigidity. Examples include a reduction of κ_η by 3 $k_\mathrm{B}T$ due to a decoration of 40% of the surface of liposomes by silica nanoparticles [48]. In stark contrast a stiffening due to nanoparticles on oil-water interfaces decreases membrane fluctuations [48]. Unlike cholesterol, nanoparticles seem to disturb the arrangement of lipids in the bilayer. Arriaga *et al*. observed a systematic increase of κ_η from 19 ± 2 $k_\mathrm{B}T$ for pure h-POPC in the L_α phase to 37 ± 2 $k_\mathrm{B}T$ at 50 mol% cholesterol, the maximum cholesterol content in a stable bilayer, by NSE and DLS [76]. The observed stiffening effect of cholesterol on h-POPC bilayers was explained assuming structural condensation caused by hydrogen-bonding complexes between the phospholipids and cholesterol in the disordered fluid phase forming an assembly of dynamical network with a net increase in mechanical properties [77, 78].

Changes induced by antimicrobial peptides like melittin on the rigidity on lipid bilayer were investigated using NSE spectroscopy [53]. The effect of pore formation of h-DOPC in HEPES buffer was studied using melittin where three distinct dynamical regimes were

observed. First, at low concentrations of melittin, as defined by peptide to lipid molar ratio, P/L = 0.2%, it is absorbed only at the surface of the membrane causing a slight decrease in the bending rigidity, κ_η. The decrease of κ_η is explained by the perturbation of chain packing by peptide adsorption [53]. Second, with increasing the concentration, pores start to form up to P/L > 1%. At a critical concentration P/L* = 0.4% about half of the LUVs are perforated. These NSE results are supported by DLS and ^{31}P NMR [53]. At the critical concentration P/L*, κ_η started to increase slightly due to high pore rigidity. Third, at higher P/L concentration, there is a rapid increase in κ_η, where the repulsive interpore interactions become significant. At P/L = 2%, the membrane fluctuations appeared to be damped by the melittin-induced pores and at P/L $\geq$ 6%, fusion of vesicles was observed [53].

A gradual increase of disordering or fluidizing of h-DMPC with increasing the concentration of nonsteroidal anti-inflammatory drugs like aspirin was observed by NSE spectroscopy [52]. A 33% decrease in bending rigidity from, κ_η = 17.4 ± 0.9 $k_\mathrm{B}T$ for pure h-DMPC to κ_η = 11.7 ± 0.4 $k_\mathrm{B}T$ for 13.5 wt% of aspirin at 20°C in the L_α phase was found. Following the X-ray diffraction studies by the Alsop *et al*. [79], it was concluded that the residence of aspirin near the head group along with increase in disorder due to the formation of gauche defects in the hydrocarbon chains is responsible for the softening or plasticizing effect of the membrane [52].

The effect of model nonsteroidal anti-inflammatory drug like ibuprofen was studied using NSE, SANS and MD simulation as a function of pH and temperature [67]. It was observed that for pure h-DMPC in the L_α phase at 30°C, the κ_η of the lipid bilayer remains relatively unchanged at high pH and decreases significantly by approximately 32%, when the pH decreases from 8 to 2. It was predicted that owing to the decrease in hydration of the lipid head group, the simultaneous decrease in κ_η has its origin in the electrostatic and structural perturbations of the lipid head [67]. It was also observed that at pH ≈ 2, κ_η decreases by ≈ 18%, for an increase in temperature from 30 to 37°C, due to the lipid chain transforming from more gel-like to more fluid-like state causing an decrease in bilayer thickness by ≈ 0.4 nm [67]. On the other hand, the introduction of Ibuprofen was found to decrease the κ_η of the lipid bilayer at all pH values, although κ_η remains unchanged with change in pH for a fixed Ibuprofen concentration [67].

Such a decrease in κ_η was explained as a combination of bilayer thinning, decrease in head group hydration and lowering of area compressibility modulus [67].

The effect of another drug like aescin on the membrane rigidity of h-DMPC liposomes in the fluid L_α phase and rigid gel $L_{\beta'}$ phase was studied by SAXS, SANS, DLS and NSE spectroscopy [54]. Saponins aescin are a type of glycosidic biosurfactants produced from plants and are used to treat diseases, like, chronic venus insufficiency (CVI), hemorrhoids and peripheral oedemic formation. From SANS a slight increase in the bilayer thickness along with increase in the radius of gyration, R_g, of the liposome was observed. SAXS reveals more prominent effects over the entire lipid thickness, where polar region of the aescin interacts with the lipid head group in the $L_{\beta'}$ phase at 10°C. In the L_α phase at 40°C insertion of the aescin deep into the bilayer thickness was observed. A decrease in κ_η in the $L_{\beta'}$ phase, whereas an increase in κ_η in the L_α phase, with increasing aescin content was reported [54]. It was concluded that the H-bond formation between the hydroxy group of aescins sugar counterpart with the carbonyl and negatively-charged phosphate groups of h-DMPC causes a reduction of κ_η in the $L_{\beta'}$ phase. In the L_α phase the incorporation of large triterpenic backbone of aescin in the bilayer causes an increase in rigidity [54].

Recently NSE spectroscopy has provided valuable information on the mechanism of lipid raft formation in liposomes. The lipid raft constitutes of a liquid ordered phase (L_O) formed from a high melting lipid like DSPC rich phase and the liquid disordered phase (L_D) formed from cholesterol forming the so called "raft" domains [49]. Using contrast variation, either the L_O or the L_D phase, can be contrast matched with the solvent [49]. Such an approach enables the extraction of bending rigidities for each the L_O and L_D phases independently. A mixture of cholesterol, DSPC and POPC in 22:39:39 ratio in a D_2O/H_2O mixture led to a diameter of the rafts of approximately 13 nm in unilamellar vesicles with a diameter of around 60 nm, as determined by separate SANS experiments. The bending modulus of the raft domains, κ_η = 126.5 ± 29.9 $k_B T$, is substantially different from that of the surrounding medium, κ_η = 18.4 ± 9.8 $k_B T$, at 20°C [49]. These values were supported by MD simulations [49]. It was concluded that this mismatch in bending moduli also accounts for the evolution of lateral heterogeneities in

different classes of lipids and in biological membranes [49]. In contrast, mixtures of h-DMPC/DSPC show a similar bending rigidity, $\kappa_\eta \approx 20\ k_B T$, as in case of the single lipid liposomes [28]. If the temperature is lowered, a substantial increase of κ_η can be observed once one of the lipids reached the gel phase (DSPC), while DMPC is still in its fluid phase [28]. It was assumed that the effective κ_η depends on the average bilayer density [28]. The variations in κ_η for different systems with and without additives are presented in table 1.

Table 1: Bending rigidity, κ_η or, $\widetilde{\kappa_\eta}$, from different papers in the L_α fluid phase. The NSE prefactor denotes the value in equation 3, used to calculate, κ_η. The last column represents the normalized κ_η from NSE to match the prefactor 0.0069.

Phospholipids in water (D_2O for NSE, H2O for other techniques)		***Lipid chains***	***T ($°C$)***	***T_m ($°C$) (methods)***	***Phase***	***Delta T= T-Tm***	***Diameter [nm]***	***κ_η (k_BT)***	***Methods***	***Prefactor in equation 3***	***κ_η (k_BT)*** *Recalculated for prefactor 0.0069 in equation 3*
10 wt % dt-DPPC		16:0 / 16:0	50	41.3 (SG) [80]	L_α	8.7	NA	46.4 ± 0.2 [10]	NSE	0.0069	46.4 ± 0.2
10 wt % dt-DSPC		18:0 / 18:0	60	54.4 (DSC) [81]	L_α	5.6	NA	49.6 ± 1.8 [10]	NSE	0.0069	49.6 ± 1.8
			65		L_α	10.6	NA	42.0 ± 1.2 [10]	NSE	0.0069	42.0 ± 1.2
			70		L_α	15.6	NA	46.4 ± 0.2 [10]	NSE	0.0069	46.4 ± 0.2
10 wt % dt-DMPC		14:0 / 14:0	30	23.6 (DSC) [81]	L_α	6.4	NA	35.6 ± 1.9 [10]	NSE	0.0069	35.6 ± 1.9
			35		L_α	11.4	NA	34.0 ± 1.8 [10]	NSE	0.0069	34.0 ± 1.8
			40		L_α	16.4	NA	30.0 ± 1.3 [10]	NSE	0.0069	30.0 ± 1.3
			50		L_α	26.4	NA	25.4 ± 1.0 [10]	NSE	0.0069	25.4 ± 1.0
			65		L_α	41.4	NA	20.6 ± 1.0 [10]	NSE	0.0069	20.6 ± 1.0
1 wt % h-DMPC		14:0 / 14:0	37	23.6 (DSC) [81]	L_α	13.4	110 [52]	17.4 ± 0.9 [52]	NSE	0.0058	24.6 ± 1.3
1 wt % h-DMPC + 13.5 wt% asprin			37		L_α	6.4	110 [52]	11.7 ± 0.9 [52]	NSE	0.0058	16.6 ± 1.3
2 wt% h-DMPC (different pH)	at pH 7.4	14:0 / 14:0	30	23.6 (DSC) [81]	L_α	6.4	100 nm pores [67]	26.2 ± 0.8 [67]	NSE	0.025	18.0 ± 0.5
	at pH 4.9				L_α	6.4	100 nm pores [67]	26.8 ± 0.9 [67]	NSE	0.025	18.4 ± 0.6
	at pH 3.3				L_α	6.4	100 nm pores [67]	24.6 ± 0.8 [67]	NSE	0.025	18.2 ± 0.5
	at pH 1.6				L_α	6.4	100 nm pores [67]	18.0 ± 0.5 [67]	NSE	0.025	12.3 ± 0.3
2 wt% h-DMPC, 31 mol% ibuprofen (different pH)	at pH 7.4		30		L_α	6.4	100 nm pores [67]	12.3 ± 0.3 [67]	NSE	0.025	8.4 ± 0.2
	at pH 4.9				L_α	6.4	100 nm pores [67]	12.8 ± 0.3 [67]	NSE	0.025	8.8 ± 0.2
	at pH 1.6				L_α	6.4	100 nm pores [67]	12.2 ± 0.3 [67]	NSE	0.025	8.4 ± 0.2
1.5 wt% h-DMPC		14:0 / 14:0	40	23.6 (DSC) [81]	L_α	16.4	100 ± 5 [54]	17 ± 0.3 [54]	NSE	0.025	11.7 ± 0.2
1.5 wt% h-	at 0.4		40	23.6	L_α	16.4	100 ± 5	26 ± 1	NSE	0.025	17.8 ± 0.7

DMPC, aescin	mol%			(DSC) [81]			[54]	[54]			
	at 0.8 mol%	14:0 / 14:0			L_α	16.4	100 ± 5 [54]	31 ± 2 [54]	NSE	0.025	21.3 ± 1.4
5 wt% h-SoyPC		16:0 / 18:2	30	-18.5 (DSC) [82]	L_α	48.5	120 ± 15 [58]	8.4 ± 1 [58]	NSE	0.0069	8.4 ± 1
5 wt% h-DOPC		18:1 / 18:1	20	-16.5 (DSC) [83]	L_α	36.5	107 ± 4 [58]	20 ± 3 [58]	NSE	0.0069	20 ± 3
10 wt% dt-DMPC/DSPC		14:0 / 14:0 and 18:0 / 18:0	15	20.5/5 0.5	$L_{\beta'}/L_{\beta'}$	-5.5/-35.5	100 nm pores [28]	124 ± 12 [28]	NSE	0.0058	175 ± 17
			25	20.5/5 0.5	$L_\alpha/L_{\beta'}$	4.5/-25.5	100 nm pores [28]	119 ± 8 [28]	NSE	0.0058	168 ± 11
			30		$L_\alpha/L_{\beta'}$	9.5/-20.5	100 nm pores [28]	120 ± 8 [28]	NSE	0.0058	169 ± 11
			35		$L_\alpha/L_{\beta'}$	14.5/-15.5	100 nm pores	61 ± 2 [28]	NSE	0.0058	86 ± 3
			40		$L_\alpha/L_{\beta'}$	19.5/-10.5	100 nm pores [28]	36 ± 2 [28]	NSE	0.0058	51 ± 3
			45		$L_\alpha/L_{\beta'}$	24.5/-5.5	100 nm pores [28]	24 ± 2 [28]	NSE	0.0058	34 ± 3
			55		L_α/L_α	34.5/4.5	100 nm pores [28]	21 ± 1 [28]	NSE	0.0058	30 ± 2
			65		L_α/L_α	44.5/14.5	100 nm pores [28]	20 ± 1 [28]	NSE	0.0058	28 ± 1
0.11 wt% h-DOPC		18:1 / 18:1	25	-16.5 (DSC) [83]	L_α	41.5	87 [48]	23 ± 1 [48]	NSE	0.0069	23 ± 1
0.11 wt% h-DOPC, 0.17 wt% Silica NPs			25		L_α	41.5	87 [48]	20 ± 1 [48]	NSE	0.0069	20 ± 1
6 mM h-DOPC (HEPES buffer)			30		L_α	46.5	92 ± 1 [53]	26.8 ± 1.6 [53]	NSE	0.0058	38 ± 2
6 mM h-DOPC (HEPES buffer) at peptide (melittin) : lipid (P/L) molar ratio (%)	P/L = 0.19		30		L_α	46.5	92 ± 1 [53]	24.9 ± 1.5 [53]	NSE	0.0058	35 ± 2
	P/L = 0.40				L_α	46.5	92 ± 1 [53]	19.1 ± 1.0 [53]	NSE	0.0058	27 ± 1
	P/L = 0.60				L_α	46.5	93 ± 1 [53]	21.4 ± 1.3 [53]	NSE	0.0058	30 ± 2
	P/L = 0.80				L_α	46.5	93 ± 1 [53]	19.8 ± 1.3 [53]	NSE	0.0058	28 ± 2
	P/L = 1.7				L_α	46.5	91 ± 1 [53]	20.6 ± 1.2 [53]	NSE	0.0058	29 ± 2

	P/L = 2.4				L_α	46.5	90.5 ± 1 [53]	28.0 ± 2.2 [53]	NSE	0.0058	40 ± 3
	P/L = 4.0	18:1 / 18:1		-16.5 (DSC) [83]	L_α	46.5	90 ± 1 [53]	42.0 ± 4.7 [53]	NSE	0.0058	59 ± 7
2 mg/ml h-POPC		16:0 / 18:1	22	-2.6 (DSC) [84]	L_α	24.6	81 ± 2 [76]	19 ± 2 [69] [76]	NSE	0.025	13.0 ± 1.4
2 mg/ml h-POPC, 50 mol% cholesterol			22		L_α	24.6	102 ± 5 [76]	37 ± 2 [76]	NSE	0.025	25.4 ± 1.4
1 mM DMPC		14:0 / 14:0	30	23.6 (DSC) [81]	L_α	6.4	NA	27.5 ± 3 [70]	Flickering	-	-
1 mM DMPC, 20 mol% cholesterol			30		L_α	6.4	NA	50.1 ± 6 [70]	Flickering	-	-
1 mM DMPC, 30 mol% cholesterol			30		L_α	6.4	NA	95.5 ± 19 [70]	Flickering	-	-
1 mM EYPC		18:1 / 16:0	30	-15 to -7[1] [85]	L_α	37 to 45	NA	27.4 ± 3.5 [70]	Flickering	-	-
1 mM G-DG		16:3 / 18:3	30	-50 (DSC/ XRD) [86]	L_α	80	NA	3.5 to 9.5 [70]	Flickering	-	-
10 mg/ml DGDG		18:3 / 18:3	room	-30 (DSC/ XRD) [86]	L_α	-	NA	2.9 ± 0.9 [71]	Flickering	-	-
10 mg/ml EYPC		18:1 / 16:0	room	-15 to -7 [85]	L_α	37 to 45	NA	19.4 ± 5 [71]	Flickering	-	-
10 mg/ml DMPE		14:0 / 14:0 PE	60	50 [87]	L_α	10	NA	15.2 ± 2 [71]	Flickering	-	-
10 mg/ml SOPC		18:0 / 18:1	18	9 (DSC) [87]	L_α	9	NA	22.5 ± 1.5 [72]	Micropipette	-	-
10 mg/ml DMPC		14:0 / 14:0	29	23.6 (DSC) [81]	L_α	5.4	NA	13.4 ± 1.4 [72]	Micropipette	-	-
10 mg/ml DAPC		20:4/ 20:4	18	-69 (DSC) [87]	L_α	87	NA	10.9 ± 1.2 [72]	Micropipette	-	-
10 mg/ml DGDG		18:3 / 18:3	23	-30 (DSC/ XRD) [86]	L_α	53	NA	10.8 ± 0.7 [72]	Micropipette	-	-
1 mg/ml SOPC		18:0 / 18:1	21	9 (DSC) [87]	L_α	12	NA	8.4 ± 0.8 [72]	Flickering	-	-
1 mg/ml DOPC		18:1 / 18:1	21	-16.5 (DSC) [83]	L_α	37.5	NA	3.9 ± 1.3 [74]	Flickering	-	-
1 mg/ml POPC		16:0 / 18:1	24	-2.6 (DSC) [84]	L_α	26.6	NA	9.5 ± 2.1 [74]	Flickering	-	-
1 mg/ml SOPC		18:0 / 18:1	21	9 (DSC) [87]	L_α	12	NA	7.9 ± 1.3 [74]	Electric Deformation	-	-
1 mg/ml DOPC		18:1 / 18:1	21	-16.5 (DSC) [83]	L_α	37.5	NA	4.2 ± 0.8 [74]	Electric Deformation	-	-

[1] EYPC is a complex mixture of phosphatidylcholines, exhibits T_m = -15 to -17 °C

1 mg/ml POPC	16:0 / 18:1	24	-2.6 (DSC) [84]	L_α	26.6	NA	14.1 ± 2.8 [74]	Electric Deformation	-	-
10 mg/ml EYPC	18:1 / 16:0	room	-15 to -7 (DSC) [85]	L_α	-	NA	6 ± 1.2 [75]	Electric Deformation	-	-
10 mg/ml DLPC	12:0 / 12:0	room	-2 (DSC) [87]	L_α	-	NA	8.2 ± 1.6 [75]	Electric Deformation	-	-
10 mg/ml DGDG	18:3 / 18:3	room	-30 (DSC/ XRD) [86]	L_α	-	NA	2.5 ± 0.5 [75]	Electric Deformation	-	-
0.2 mg/ml POPC	16:0 / 18:1	20	-2.6 (DSC) [84]	L_α	22.6	20-50 μm [38]	39.52 ± 0.7 [38]	Flickering	-	-
0.2 mg/ml POPC in HEPES buffer		20		L_α	22.6	20-50 μm [38]	39.09 ± 0.7 [38]	Flickering	-	-
0.2 mg/ml POPC in Histidine buffer		20		L_α	22.6	20-50 μm [38]	40.61 ± 0.4 [38]	Flickering	-	
0.2 mg/ml POPC in MES buffer		20		L_α	22.6	20-50 μm [38]	33.07 ± 0.4 [38]	Flickering	-	
0.2 mg/ml POPC in MOPS buffer		20		L_α	22.6	20-50 μm [38]	34.70 ± 0.7 [38]	Flickering	-	
0.2 mg/ml POPC in PIPES buffer		20		L_α	22.6	20-50 μm [38]	37.98 ± 1.0 [38]	Flickering	-	
0.2 mg/ml POPC in TRIS buffer		20		L_α	22.6	20-50 μm [38]	35.79 ± 0.4 [38]	Flickering	-	
0.2 mg/ml POPC in 100 mM NaCl		20		L_α	22.6	20-50 μm [38]	31.01 ± 0.8 [38]	Flickering	-	
0.2 mg/ml POPC in 100 mM NaCl, 2 mM EDTA, 10 mM TRIS		20		L_α	22.6	20-50 μm [38]	24.00 ± 0.3 [38]	Flickering	-	
0.2 mg/ml POPC in 100 mM NaCl, 10 mM TRIS		20		L_α	22.6	20-50 μm [38]	24.62 ± 1.2 [38]	Flickering	-	

5.3. Thickness Fluctuations of the Bilayer

In addition to undulations, (spontaneous) fluctuations of the thickness of the bilayer were proposed theoretically in the early 1980s [88-91] and are considered to be the primary mechanism underlying pore formation in membranes [92, 93], which leads to passive permeability of the membrane for drugs [94]. The amplitude of the fluctuations is around 3.7 Å, and seems to be less dependent on the length of the alkyl chains, at least for a variation from 14 to 18 carbon atoms in the fatty acid tails [27]. The relaxation occurs well in the time window of NSE and seems to have characteristic fluctuation times on the order of 100 ns [27], which is the same order of magnitude at which conformational transitions in proteins occur [95].

Since all protons contribute to the signal and overshadow the information on thickness fluctuations of the bilayer, Woodka *et al.* employed partially deuterated and fully hydrogenated

DMPC, DPPC, and DSPC [27]. In this pioneering study the time-dependent structural correlations between the head groups were studied by contrast matching of the tail by the solvent [27]. Thickness fluctuations seem to be very common in soft matter and biological systems. For example, Farago *et al.* reported the occurrence of similar processes in the lamellae of SDS-water-penthanol-dodecane microemulsions in the lyotropic phase [96].

In order to describe the observations by the ZG model, a semi-empirical approach was introduced that accounts for the additional Q-dependence of the decay rate Γ_q/Q^3 due to the structural correlations [10, 27, 97]

$$\frac{\Gamma_q}{Q^3} = \frac{\Gamma_{ZG}}{Q^3} + \frac{1}{\tau_{TF} Q_0^3}\left[\frac{1}{1 + (Q - Q_0)^2 \xi^2}\right] \quad (5)$$

The second term introduces the relaxation time of the thickness fluctuations, τ_{TF}. The thickness of the bilayer can be obtained from the position, Q_0, of the structural correlation of the head groups. The amplitude of the fluctuations in the reciprocal space is described by the parameter ξ^{-1}.

As illustrated in figure 3 a, SAXS and SANS studies on DMPC, DPPC and DSPC show the minimum at $Q = Q_0$ is determined by the bilayer thickness only, whereas the peak at $Q > Q_0$ reflects both the bilayer thickness and thickness fluctuation amplitude of the membrane [98]. As summarized by figure 2b, from the modeling of NSE data with equation 2 the Q-dependence of the decay rate Γ_q/Q^3 shows a distinct peak close to Q_0 in case of the tail contrast matched samples. The solid lines represent the calculations by equation 4. Differences between the full contrast experiments – tail and heads visible in case of hydrogenated (h) lipids in D_2O – and tail deuterated (dt) samples is obvious. This peak is a direct evidence of the substantial contribution of a process in addition to the ZG behavior and is ascribed to the thickness fluctuations [28].

(a) (b)

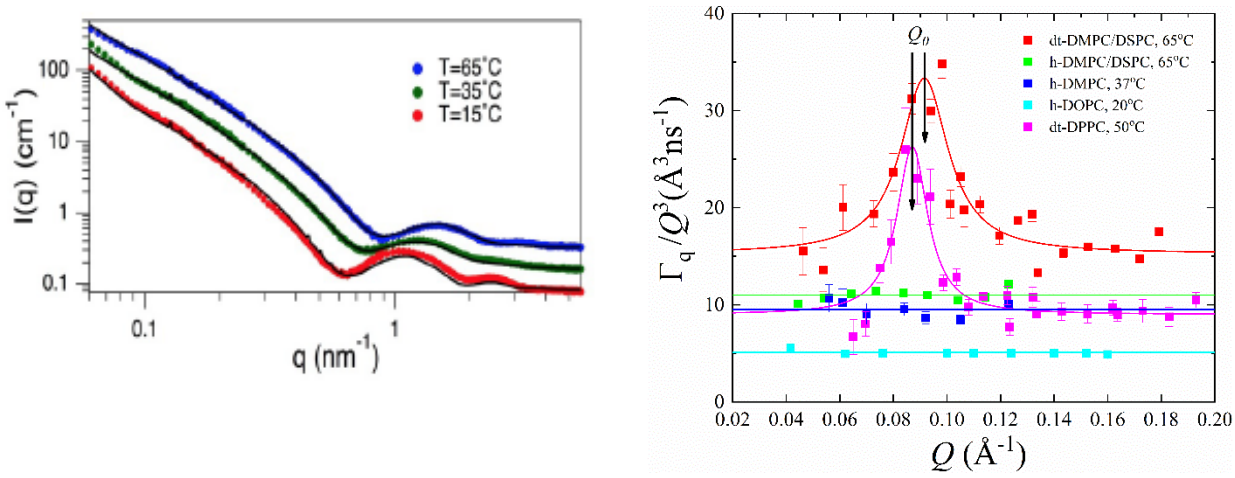

Figure 3. *(a) SANS scattering diagrams on dt-DMPC/dt-DSPC at three different temperatures. Reproduced from the literature [28]. (b) The decay rate, Γ_q/Q^3, from NSE relaxation spectrum for tail-deuterated (dt) and fully hydrogenated (h) phospholipids in the fluid phase. The solid lines represent calculated results by equation 4. The data for h-DMPC [52], h-DOPC [58], dt-DPPC [27] and the lipid mixtures dt-DMPC (41.5wt%)/dt-DSPC (48.3wt%) in h-DMPC (4.49wt%)-h-DSPC (1.1wt%), and, h-DMPC (46.1wt%)/h-DSPC (53.8wt%) [28] are adapted from the literature.*

Recently, Bingham *et al.* [99] introduced a theoretical relation between thickness fluctuations and viscoelastic properties of membranes. Following that prediction Nagao *et al.* [10] have included both the elastic and viscous components in the Lorentzian expression as

$$\frac{\Gamma_q}{Q^3} = \frac{\Gamma_{ZG}}{Q^3} + \frac{K_A k_B T}{\mu Q_0^3 k_B T + 4\mu Q_0 K_A A_0 (Q - Q_0)^2} \qquad (6)$$

Here K_A is the area compressibility modulus, A_0 is the area per lipid molecule and μ is the local viscosity of the membrane. The obtained membrane viscosity was found to decrease with increase in temperature for DMPC, DPPC and DSPC, ranging from 10 to 100 nPa·s [10]. The most important consequence of equation 6 is the connection of the viscoelastic properties of the membrane with the bending and thickness fluctuations. Generically speaking, the viscosity of lipid membranes seem to vary from 1 to 700 nPa·s·m. Nagao report a linear increase with

temperature and the results suggest that values of around 100 nPa·s·m are reached at T_m for DMPC, DPPC, DSPC [10].

5.4. Lipid Lateral Motions

Lipid lateral motion embraces all time-dependent processes perpendicular to the symmetry axis of the lipids. These may include independent motion of single lipids or groups of lipids, or collective dynamics. Hereafter, we consider only motions of those lipids confined to one leaflet of the bilayer and omit flip-flop processes, which will be discussed in section 6.7. Mode coupling theory and MD simulations indicate that the lateral motion of the lipid entity (head and tail) is restricted by cages formed by neighboring lipids [100]. In addition, MD simulations predict a sub-diffusive motion of the lipids due to the crowded environment that leads to a non-Gaussian dynamics [101].

Several experimental techniques permit the measurement of lateral motions at different length- and time-scales. Busch *et al.* used quasielastic neutron scattering (QENS) to access the fast-localized motion of h-DMPC lipid molecules at time-scale from few ps to few ns [29]. The authors conclude that the entire lipid molecules undergo localized diffusive motions along with its neighbors [29, 102]. In agreement with MD simulations they found the lipid molecules form a dynamically assembling patch [29, 102]. A more detailed study of the lateral diffusion was conducted by Sharma *et al*. on h-DMPC [52, 103, 104] using QENS. They authors used a separation ansatz to distinguish the lateral from the faster internal motion. It was concluded that D_{lat} is essentially determined by three contributions, the change in free volume, f_{fv}, direct obstructions, f_{obst}, and interactions, f_{int}, between the additives and lipids [103]. Recently, more details have been obtained extracting the mean square displacement by a procedure established earlier. It shows a certain motion of the tails, which can be considered as a trapped motion of the tails [105-107].

A very successful tool to measure lateral diffusion is fluorescence recovery after photo bleaching (FRAP). Fluorescent molecules are embedded in the bilayer and bleached in one region. By recovery of the fluorescence intensity, Brownian motion of the fluorescent molecules (lateral

diffusion) is quantified [108]. Under such circumstances, microscopes can be used to track the motion of organic fluorophores, typically on a time- and length-scale of ms to s and mm-μm, respectively. Typical diffusion coefficients of around 0.67 – 1.62 $Å^2ns^{-1}$ are obtained [109], values which are well compatible with those obtained by other techniques, such as QENS, PFG NMR and RET, cf. table 2. PFG-NMR has been extensively used to explore lateral diffusion [110]. Most of the studies concentrate on oriented bilayers, powders or hydrated multilamellar structure, which are omitted here. Astonishingly only a few attempts target the lateral diffusion of lipids in spherical liposomes ins the liquid, L_α, phase.

The effect of additives like cholesterol, myristic acid, farnesol, and sodium glycocholate on the lateral dynamics of h-DMPC was studied using QENS [111] [104]. While a decrease of the lipid lateral mobility of h-DMPC with increasing cholesterol content was observed, the other additives did not significantly impact the mobility of lipids [104] [111]. It was concluded that cholesterol affects the packing density of the tail regime causing a decrease of free volume, and thereby lowering the overall in-plane lipid mobility [111]. Observations of enhanced membrane rigidities (table 1) may also be associated with a closer packing of lipids.

A systematic study of the impact of the addition of antimicrobial peptides alamethicin and melittin on the dynamics of h-DMPC by QENS in the L_α fluidic phase discovered a reduced lateral diffusion and a stiffening of the membrane, with melittin being a stronger stiffening agent than alamethicin [103]. For comparison, at T = 6.85 °C and 19.85 °C, both are in the $L_{\beta'}$ gel phase, there was no change in the lateral diffusion on addition of alamethicin, however there is an increase in D_{lat} on addition of melittin (table 2). The addition of cholesterol decreases the mobility of h-DMPC [111] and lowers the binding affinity of melittin to the bilayer, but also saturates the liposomes that prohibits further incorporation of melittin into the bilayer [104]. In this case, D_{lat} is not affected by the addition of melittin as observed in table 2. On the other hand, addition of drugs like, aspirin causes a slight increase in D_{lat} both in $L_{\beta'}$ and L_α phases in h-DMPC due to the plasticizing effect of aspirin [52], causing a decrease in the membrane rigidity as observed before (table 1).

Table 2: Comparison between values of lateral diffusion coefficient, D_{lat}, from different techniques, for the L_{α} fluid and $L_{\beta'}$ gel phases.

Phospholipids in water (D_2O for QENS)	***T (° C)***	**Lipid Phase**	***D_{lat} (Å^{2}ns^{-1})***	***Methods***

100 mM h-DMPC	6.85	$L_{\beta'}$	0.7 ± 0.1 [103]	QENS
	19.85	$L_{\beta'}$	1.4 ± 0.1 [103]	QENS
	36.85	L_{α}	5.0 ± 0.2 [103]	QENS
100 mM h-DMPC, 0.5 mol% alamethicin	6.85	$L_{\beta'}$	0.7 ± 0.1 [103]	QENS
	19.85	$L_{\beta'}$	1.3 ± 0.1 [103]	QENS
	36.85	L_{α}	4.9 ± 0.1 [103]	QENS
100 mM h-DMPC, 0.5 mol% melittin	6.85	$L_{\beta'}$	1.2 ± 0.1 [103]	QENS
	19.85	$L_{\beta'}$	1.9 ± 0.1 [103]	QENS
	36.85	L_{α}	3.3 ± 0.1 [103]	QENS
7wt% h-DMPC	19.85	$L_{\beta'}$	1.5 ± 0.1 [52]	QENS
	36.85	L_{α}	6.0 ± 0.1 [52]	QENS
7wt% h-DMPC, 6.5 wt% asprin	19.85	$L_{\beta'}$	2.5 ± 0.1 [52]	QENS
	36.85	L_{α}	6.3 ± 0.1 [52]	QENS
74 mM h-DMPC	19.85	$L_{\beta'}$	0.7 ± 0.1 [104]	QENS
	36.85	L_{α}	7.7 ± 0.3 [104]	QENS
74 mM h-DMPC, 0.2 mol% melittin	19.85	$L_{\beta'}$	1.1 ± 0.1 [104]	QENS
	36.85	L_{α}	2.4 ± 0.1 [104]	QENS
74 mM h-DMPC, 20 mol% cholesterol	19.85	$L_{\beta'}$	0.7 ± 0.1 [104]	QENS
	36.85	L_{α}	2.8 ± 0.1 [104]	QENS
74 mM h-DMPC, 0.2 mol% melittin, 20 mol% cholesterol	19.85	$L_{\beta'}$	0.7 ± 0.1 [104]	QENS
	36.85	L_{α}	2.8 ± 0.1 [104]	QENS
12wt% h-POPC in H_2O (MLV)	48.85	L_{α}	1.9 ± 0.1 [110]	PFG-MAS
BOD diffusion in h-DMPC (MLV)	27	L_{α}	0.67 – 1.62 [109]	FRAP
h-DMPG (ULV) in H_2O	10	L_{α}	0.04 [112]	RET

	23	L_α	0.11 [112]	RET
	35	L_α	0.23 [112]	RET
h-DOPC (ULV) in H_2O	10	L_α	0.31 [112]	RET
	23	L_α	0.69 [112]	RET
	35	L_α	1.6 [112]	RET
3wt% h-DPPC	25	L_α	0.68 [113]	PFG - NMR

5.5. Lipid rotational motion

The notion lipid rotational motion embraces several possible processes [114]. Considering lipids as circular cylindrical entities, (i) rotations around their symmetry axes, which is assumed to be perpendicular to the bilayer plane (axial rotation), can occur. While free lipids could also rotate around their longitudinal axes, the bilayer restricts this attempt to a confined space (wobbling). The term anisotropic diffusion embraces axial rotation [5] and wobbling [115]. Lipids are flexible molecules, in which the (iii) lipid head group and fatty acid tails may show a different rotational motion from the entity. Furthermore, (iv) tails may rotate (flexing) (lipid hydro-carbon chain as an entity), but also the rotational isomerization around C-C bonds.

Axial rotation of phospholipids can be measured using several techniques (Dielectric spectroscopy, ESR and NMR) [116] [5]. Roberts and Redfield identified molecular rotation and wobbling by ^{31}P Field Cycling NMR experiments [115]. A more recent study of Klauda *et al.* shows how the ^{31}P field cycling NMR data agrees with molecular dynamic simulations while the dynamics are described by a rigid-body model [117]. In fluid phase, cumulative effect of the rotational isomerism of C-C bonds in the fatty acid chains gives rise to a shorter length of the fatty acid chain and as well as more disordered structure. These individual rotations around C-C bonds are in fact crucial in obtaining the fluid phase of bio membranes.

5.6. Lipid flip-flop motion

The notions flip-flop or transverse diffusion of lipids refer to the change of lipids from one to the other bilayer. Many biological membranes maintain distinct asymmetry between the inner and

outer monolayers of the bilayer in terms of lipid composition. This could only be explained by a transverse movement of lipids although it seems energetically unfavorable [118]. In cells, this movement is controlled enzymatically by energy driven or independent flippases (inward movement) and floppases (outward movement) [119].

A direct method of measuring the flip-flop motion in fluid phase vesicles is by using Electron Paramagnetic Resonance (EPR) [120]. Fluorescence spectroscopy has shown detergents can accelerate flip dynamics in fluorescence labelled erythrocytes [121]. However, it has been observed that using fluorescent or spin-labelled lipids do not accurately represent the native lipid flip-flop dynamics [122]. Therefore, it is important to explore techniques that obtain flip-flop dynamics without or minimum perturbation to the lipid bilayer. Recently, Marquardt et.al. have studied translocation rates in DPPC vesicles in both gel and fluid phases under various temperatures using ^{1}H NMR coupled with a paramagnetic shift reagent where they found that in the gel phase translocation is much slower compared to fluid phase [123]. Molecular dynamics simulations have provided important insights on flip-flop dynamics in relationship to water permeation, acyl chain length and unsaturation, integral membrane proteins and the presence of cholesterol [124] [125-127]. Time–resolved SANS on DMPC, POPC and POPA vesicles have shown that acyl chain length and saturation change the flip-flop motion rates. Moreover, it has also shown cholesterol entirely inhibits flip-flop in DMPC vesicles [128]. SANS have also been employed in showing that methanol can increase the rate of flip-flop in DMPC LUVs in fluid phase [129].

6. Future perspectives

This review summarizes the dynamics of liposomes. A variety of processes can be envisioned. In many cases, differences in time- and/or length-scale can help to distinguish them from each other. In order to understand how the molecular mechanisms may contribute to the membrane properties at least 12 orders of magnitude need to be captured to track the dynamics from the motion of single elements (~ 0.9 nm) to the translational diffusion of liposomes (~ 20 nm to several μm for LUVs). Numerous experimental and simulation techniques are necessary to capture such a broad time- and length scale range.

We have discussed in detail the rich morphology of the liposomes and the different dynamics of the liposomes over a broad length and time scale. In order to understand the dynamics at different time scales one needs to consider specific techniques. We have shown that scattering experiments like SANS and SAXS are vital to understand the structure and morphology of the liposomes, whereas, neutron spectroscopic techniques like NSE and QENS are vital to understand the membrane fluctuations (undulation), thickness fluctuations and lipid lateral motions in nano to picosecond time scale. The length scale dependent dynamics measured from different scattering techniques are noteworthy to validate different scaling behavior from theory and simulations. Other techniques like, DLS and PFG-NMR provides us valuable information about the center of mass diffusion of the liposome in millisecond time scale. The lipid rotational motion was successfully perturbed using Dielectric spectroscopy, ESR and NMR. The slower flip-flop motion of the lipid can be best measured using EPR techniques. Understanding the dynamics of lipid bilayer is gaining more importance in order to tune the viscoelastic properties of the lipid bilayer. In this context a joint study of NSE and QENS is very important.

7. Acknowledgments

The neutron scattering work is supported by the U.S. Department of Energy (DOE) under EPSCoR Grant No. DE-SC0012432 with additional support from the Louisiana Board of Regents. This paper was prepared as an account of work sponsored by an agency of the United States Government. Neither the United States Government nor any agency thereof, nor any of their employees, makes any warranty, express or implied, or assumes any legal liability or responsibility for the accuracy, completeness, or usefulness of any information, apparatus, product, or process disclosed, or represents that its use would not infringe privately owned rights. Reference herein to any specific commercial product, process, or service by trade name, trademark, manufacturer, or otherwise does not necessarily constitute or imply its endorsement, recommendation, or favoring by the United States Government or any agency thereof. The views and opinions of authors expressed herein do not necessarily state or reflect those of the United States Government or any agency thereof.

References

• of special interest.
[14] The authors identified phase separation within the fluid membrane can lead to domain induced budding.
[48] The authors observed reduction in membrane rigidity on adhesion of silica nanoparticle by NSE.
[51] The authors for the first time related thickness fluctuation with bilayer thickness
[54] For the first time identifies a decrease in κ_η in the $L_{\beta'}$ phase, whereas an increase in κ_η in the L_α phase, with increasing aescin content was reported.
[58] First time observation of localized dynamics within NSE time window
[67] First observation of the effect of pH and ibuprofen on the bending rigidity
[76] First stiffening effect of cholesterol in the L_α phase of lipid bilayer
[103] The authors proved that the disruption of lateral motions in the lipid bilayer by QENS, but not the pore formation due to peptides is the principal interaction.
[112] Lateral diffusion in membranes was measured by resonance energy transfer
[123] Detailed description of the flip-flop motions in the gel and fluid phase by ^{1}H-NMR
First time showed that the acyl chain length and headgroup size determines the flip-flop motions by time-resolved SANS.

•• of outstanding interest.
[10] The authors for the first time calculated membrane viscosity from NSE.
[12] The authors for the first time calculated the curvature energy for membranes.
[13] The authors for the first time theoretically proposed different morphologies of vesicles.
[22] First joint refinement of x-ray and neutron diffraction data to understand the distribution of molecules in the lipid bilayer.
[27] The authors for the first time discovered thickness fluctuations in lipid bilayers
[29] The authors for the first time identified lateral motions from QENS data
[49] The authors for the first time identified that the rigidity of the lipid rafts are different than the sarrounding lipids using contrast variantion NSE.
[53] First systematic observation of pore formations in lipid bilayer and the corresponding rigidity.
[56] First theoretical prediction of membrane undulation
[120] First direct measurement of flip-flop motions in the L_α phase by EPR

[1] Bonifacino JS, Glick BS. The Mechanisms of Vesicle Budding and Fusion. Cell. 2004;116:153-66.
[2] Storck EM, Ozbalci C, Eggert US. Lipid Cell Biology: A Focus on Lipids in Cell Division. Annu Rev Biochem. 2018;87:839-69.
[3] McCusker D, Kellogg DR. Plasma membrane growth during the cell cycle: unsolved mysteries and recent progress. Curr Opin Cell Biol. 2012;24:845-51.
[4] Bernsdorff C, Wolf A, Winter R, Gratton E. Effect of hydrostatic pressure on water penetration and rotational dynamics in phospholipid-cholesterol bilayers. Biophysical Journal. 1997;72:1264-77.

[5] Aguilar LF, Pino JA, Soto-Arriaza MA, Cuevas FJ, Sánchez S, Sotomayor CP. Differential Dynamic and Structural Behavior of Lipid-Cholesterol Domains in Model Membranes. PLOS ONE. 2012;7:e40254.
[6] Menon AK, Herrmann A. Lipid Flip-Flop. In: Roberts GCK, editor. Encyclopedia of Biophysics. Berlin, Heidelberg: Springer Berlin Heidelberg; 2013. p. 1261-4.
[7] Andaloussi SE, Mager I, Breakefield XO, Wood MJ. Extracellular vesicles: biology and emerging therapeutic opportunities. Nat Rev Drug Discov. 2013;12:347-57.
[8] Nikoleli GP, Nikolelis DP, Siontorou CG, Karapetis S, Nikolelis MT. Application of Biosensors Based on Lipid Membranes for the Rapid Detection of Toxins. Biosensors (Basel). 2018;8.
[9] Lipowsky R, Sackmann E. Structure and Dynamics of Membranes, From Cells to Vesicles. 1st ed: North Holland; 1995.
[10] Nagao M, Kelley EG, Ashkar R, Bradbury R, Butler PD. Probing Elastic and Viscous Properties of Phospholipid Bilayers Using Neutron Spin Echo Spectroscopy. J Phys Chem Lett. 2017:4679-84.
[11] Katsaras J, Gutberlet T. Lipid Bilayers: Structure and Interactions. Berlin, Heidelberg,: Springer-Verlag; 2001.
[12] Helfrich W. Elastic Properties of Lipid Bilayers: Theory and Possible Experiments. Z Naturforsch. 1973;28c:693-703.
[13] Seifert U, Berndl K, Lipowsky R. Shape transformations of vesicles: Phase diagram for spontaneous- curvature and bilayer-coupling models. Physical Review A. 1991;44:1182-202.
[14] Julicher F, Lipowsky R. Domain-induced budding of vesicles. Phys Rev Lett. 1993;70:2964-7.
[15] Seifert U. Curvature-induced lateral phase segregation in two-component vesicles. Phys Rev Lett. 1993;70:1335-8.
[16] Käs J, Sackmann E. Shape transitions and shape stability of giant phospholipid vesicles in pure water induced by area-to-volume changes. Biophysical Journal. 1991;60:825-44.
[17] Käs J, Sackmann E, Podgornik R, Svetina S, Žekš B. Thermally induced budding of phospholipid vesicles — a discontinuous process. Journal de Physique II. 1993;3:631-45.
[18] Döbereiner HG, Käs J, Noppl D, Sprenger I, Sackmann E. Budding and fission of vesicles. Biophysical Journal. 1993;65:1396-403.
[19] Nagle JF. Introductory Lecture: Basic quantities in model biomembranes. Faraday Discuss. 2013;161:11-29.
[20] Nagle JF, Tristram-Nagle S. Structure of lipid bilayers. Biochimica et Biophysica Acta (BBA) - Reviews on Biomembranes. 2000;1469:159-95.
[21] Frielinghaus H. Small-angle scattering model for multilamellar vesicles. Phys Rev E Stat Nonlin Soft Matter Phys. 2007;76:051603.
[22] Wiener MC, White SH. Structure of a fluid dioleoylphosphatidylcholine bilayer determined by joint refinement of x-ray and neutron diffraction data. III. Complete structure. Biophysical Journal. 1992;61:434-47.
[23] Ananthapadmanabhan KP, Goddard ED, Turro NJ, Kuo PL. Fluorescence Probes for Critical Micelle Concentration. Langmuir. 1985;1:352-5.
[24] Marsh D. Handbook of Lipid Bilayers 2nd ed: CRC Press; 2013.
[25] Dufourc EJ. Sterols and membrane dynamics. Journal of Chemical Biology. 2008;1:63-77.
[26] Berndl K, Käs J, Lipowsky R, Sackmann E, Seifert U. Shape Transformations of Giant Vesicles: Extreme Sensitivity to Bilayer Asymmetry. Europhysics Letters (EPL). 1990;13:659-64.

[27] Woodka AC, Butler PD, Porcar L, Farago B, Nagao M. Lipid bilayers and membrane dynamics: insight into thickness fluctuations. Phys Rev Lett. 2012;109:058102.
[28] Ashkar R, Nagao M, Butler PD, Woodka AC, Sen MK, Koga T. Tuning membrane thickness fluctuations in model lipid bilayers. Biophys J. 2015;109:106-12.
[29] Busch S, Smuda C, Pardo LC, Unruh T. Molecular mechanism of long-range diffusion in phospholipid membranes studied by quasielastic neutron scattering. J Am Chem Soc. 2010;132:3232-3.
[30] Singer SJ, Nicolson GL. The Fluid Mosaic Model of the Structure of Cell Membranes. Science. 1972;175:720.
[31] Blume A. Properties of lipid vesicles: FT-IR spectroscopy and fluorescence probe studies. Current Opinion in Colloid & Interface Science. 1996;1:64-77.
[32] Bloom M, Evans E. Observation of Surface Undulations on the Mesoscopic Length Scale by NMR. In: Peliti L, editor. Biologically Inspired Physics. Boston, MA: Springer US; 1991. p. 137-47.
[33] Bloom M, Evans E, Mouritsen OG. Physical properties of the fluid lipid-bilayer component of cell membranes: a perspective. Quarterly Reviews of Biophysics. 2009;24:293-397.
[34] Wanderlingh U, D'Angelo G, Branca C, Conti Nibali V, Trimarchi A, Rifici S, et al. Multi-component modeling of quasielastic neutron scattering from phospholipid membranes. The Journal of Chemical Physics. 2014;140:174901.
[35] Frey L, Hiller S, Riek R, Bibow S. Lipid- and Cholesterol-Mediated Time-Scale-Specific Modulation of the Outer Membrane Protein X Dynamics in Lipid Bilayers. Journal of the American Chemical Society. 2018;140:15402-11.
[36] Lenaz G. Lipid fluidity and membrane protein dynamics. Bioscience Reports. 1987;7:823.
[37] Klauda JB, Roberts MF, Redfield AG, Brooks BR, Pastor RW. Rotation of Lipids in Membranes: Molecular Dynamics Simulation, ³¹P Spin-Lattice Relaxation, and Rigid-Body Dynamics. Biophysical Journal. 2008;94:3074-83.
[38] Bouvrais H, Duelund L, Ipsen JH. Buffers Affect the Bending Rigidity of Model Lipid Membranes. Langmuir. 2014;30:13-6.
[39] Andar AU, Hood RR, Vreeland WN, Devoe DL, Swaan PW. Microfluidic preparation of liposomes to determine particle size influence on cellular uptake mechanisms. Pharm Res. 2014;31:401-13.
[40] Batchelor GK. Diffusion in a dilute polydisperse system of interacting spheres. Journal of Fluid Mechanics. 2006;131.
[41] Cichocki B, Felderhof BU. Diffusion of Brownian particles with hydrodynamic interaction and hard core repulsion. The Journal of Chemical Physics. 1991;94:556-62.
[42] Gupta S, Stellbrink J, Zaccarelli E, Likos CN, Camargo M, Holmqvist P, et al. Validity of the Stokes-Einstein Relation in Soft Colloids up to the Glass Transition. Phys Rev Lett. 2015;115:128302.
[43] Odeh F, Heldt N, Gauger M, Slack G, Li Y. PFG-NMR Investigation of Liposome Systems Containing Hydrotrope. Journal of Dispersion Science and Technology. 2006;27:665-9.
[44] Leal C, Rögnvaldsson S, Fossheim S, Nilssen EA, Topgaard D. Dynamic and structural aspects of PEGylated liposomes monitored by NMR. Journal of Colloid and Interface Science. 2008;325:485-93.
[45] Lipowsky R. The conformation of membranes. Nature. 1991;349:475.

[46] Safinya CR, Sirota EB, Roux D, Smith GS. Universality in interacting membranes: The effect of cosurfactants on the interfacial rigidity. Phys Rev Lett. 1989;62:1134-7.
[47] Evan Evans, David Needham. Physical properties of surfactant bilayer membranes: thermal transitions, elasticity, rigidity, cohesion and colloidal interactions. Journal of Physical Chemistry. 1987;91:4219-28.
[48] Hoffmann I, Michel R, Sharp M, Holderer O, Appavou MS, Polzer F, et al. Softening of phospholipid membranes by the adhesion of silica nanoparticles--as seen by neutron spin-echo (NSE). Nanoscale. 2014;6:6945-52.
[49] Nickels JD, Cheng X, Mostofian B, Stanley C, Lindner B, Heberle FA, et al. Mechanical Properties of Nanoscopic Lipid Domains. J Am Chem Soc. 2015;137:15772-80.
[50] Bradbury R, Nagao M. Effect of charge on the mechanical properties of surfactant bilayers. Soft Matter. 2016;12:9383-90.
[51] Nagao M, Chawang S, Hawa T. Interlayer distance dependence of thickness fluctuations in a swollen lamellar phase. Soft Matter. 2011;7.
[52] Sharma VK, Mamontov E, Ohl M, Tyagi M. Incorporation of aspirin modulates the dynamical and phase behavior of the phospholipid membrane. Phys Chem Chem Phys. 2017;19:2514-24.
[53] Lee JH, Choi SM, Doe C, Faraone A, Pincus PA, Kline SR. Thermal fluctuation and elasticity of lipid vesicles interacting with pore-forming peptides. Phys Rev Lett. 2010;105:038101.
[54] Sreij R, Dargel C, Geisler P, Hertle Y, Radulescu A, Pasini S, et al. DMPC vesicle structure and dynamics in the presence of low amounts of the saponin aescin. Phys Chem Chem Phys. 2018;20:9070-83.
[55] Holler S, Moreno AJ, Zamponi M, Bačová P, Willner L, Iatrou H, et al. The Role of the Functionality in the Branch Point Motion in Symmetric Star Polymers: A Combined Study by Simulations and Neutron Spin Echo Spectroscopy. Macromolecules. 2017;51:242-53.
[56] Zilman AG, Granek R. Undulations and Dynamic Structure Factor of Membranes. Phys Rev Lett. 1996;77:4788-91.
[57] Watson MC, Brown FL. Interpreting membrane scattering experiments at the mesoscale: the contribution of dissipation within the bilayer. Biophys J. 2010;98:L9-L11.
[58] Gupta S, De Mel JU, Perera RM, Zolnierczuk P, Bleuel M, Faraone A, et al. Dynamics of Phospholipid Membranes beyond Thermal Undulations. J Phys Chem Lett. 2018;9:2956-60.
[59] Kandil ME, Harris KR, Goodwin ARH, Hsu K, Marsh KN. Measurement of the Viscosity and Density of a Reference Fluid, with Nominal Viscosity atT= 298 K andp= 0.1 MPa of 29 mPa·s, at Temperatures between (273 and 423) K and Pressures below 275 MPa. Journal of Chemical & Engineering Data. 2006;51:2185-96.
[60] Takeda T, Kawabata Y, Seto H, Komura S, Ghosh SK, Nagao M, et al. Neutron spin–echo investigations of membrane undulations in complex fluids involving amphiphiles. Journal of Physics and Chemistry of Solids. 1999;60:1375-7.
[61] Hoffmann I, Hoffmann C, Farago B, Prevost S, Gradzielski M. Dynamics of small unilamellar vesicles. J Chem Phys. 2018;148:104901.
[62] Milner ST, Safran SA. Dynamical fluctuations of droplet microemulsions and vesicles. Physical Review A. 1987;36:4371.

[63] Brodeck M, Maccarrone S, Saha D, Willner L, Allgaier J, Mangiapia G, et al. Asymmetric polymers in bicontinuous microemulsions and their accretion to the bending of the membrane. Colloid and Polymer Science. 2014;293:1253-65.
[64] Lipfert F, Holderer O, Frielinghaus H, Appavou MS, Do C, Ohl M, et al. Long wavelength undulations dominate dynamics in large surfactant membrane patches. Nanoscale. 2015;7:2578-86.
[65] Monkenbusch M, Holderer O, Frielinghaus H, Byelov D, Allgaier J, Richter D. Bending moduli of microemulsions; comparison of results from small angle neutron scattering and neutron spin-echo spectroscopy. Journal of Physics: Condensed Matter. 2005;17:S2903-S9.
[66] Ahmadpoor F, Sharma P. Thermal fluctuations of vesicles and nonlinear curvature elasticity--implications for size-dependent renormalized bending rigidity and vesicle size distribution. Soft Matter. 2016;12:2523-36.
[67] Boggara MB, Faraone A, Krishnamoorti R. Effect of pH and Ibuprofen on the Phospholipid Bilayer Bending Modulus. The Journal of Physical Chemistry B. 2010;114:8061-6.
[68] Mell M, Moleiro LH, Hertle Y, Fouquet P, Schweins R, Lopez-Montero I, et al. Bending stiffness of biological membranes: what can be measured by neutron spin echo? Eur Phys J E Soft Matter. 2013;36:75.
[69] Arriaga LR, Lopez-Montero I, Orts-Gil G, Farago B, Hellweg T, Monroy F. Fluctuation dynamics of spherical vesicles: frustration of regular bulk dissipation into subdiffusive relaxation. Phys Rev E Stat Nonlin Soft Matter Phys. 2009;80:031908.
[70] H.P. Duwe, J. Kaes, E. Sackmann. Bending elastic moduli of lipid bilayers : modulation by solutes. Journal de Physique France. 1990;51:945-61.
[71] M. Mutz, W. Helfrich. Bending rigidities of some biological model membranes as obtained from the Fourier analysis of contour sections. Journal de Physique France. 1990;51:991-1001.
[72] Evans E, Rawicz W. Entropy-driven tension and bending elasticity in condensed-fluid membranes. Phys Rev Lett. 1990;64:2094-7.
[73] Rawicz W, Olbrich KC, McIntosh T, Needham D, Evans E. Effect of Chain Length and Unsaturation on Elasticity of Lipid Bilayers. Biophysical Journal. 2000;79:328-39.
[74] Niggemann G, Kummrow M, Helfrich W. The Bending Rigidity of Phosphatidylcholine Bilayers: Dependences on Experimental Method, Sample Cell Sealing and Temperature. Journal de Physique II France. 1995;5:413-25.
[75] Kummrow M, Helfrich W. Deformation of giant lipid vesicles by electric fields. Physical Review A. 1991;44:8356-60.
[76] Arriaga LR, Lopez-Montero I, Monroy F, Orts-Gil G, Farago B, Hellweg T. Stiffening effect of cholesterol on disordered lipid phases: a combined neutron spin echo + dynamic light scattering analysis of the bending elasticity of large unilamellar vesicles. Biophys J. 2009;96:3629-37.
[77] Ole G. Mouritsen, Kent Jørgensen. Dynamical order and disorder in lipid bilayers. Chemistry and Physics of Lipids. 1994;73:3-25.
[78] Presti FT. The role of cholesterol in membrane fluidity. In Membrane Fluidity in Biology. New York: Academic Press; 1985.
[79] Alsop RJ, Maria Schober R, Rheinstadter MC. Swelling of phospholipid membranes by divalent metal ions depends on the location of the ions in the bilayers. Soft Matter. 2016;12:6737-48.

[80] Biltonena RL, Lichtenberg D. The use of differential scanning calorimetry as a tool to characterize liposome preparations. Chemistry and Physics of Lipids. 1993;64:129.
[81] Lewis RNAH, Mak N, McElhaney RN. A differential scanning calorimetric study of the thermotropic phase behavior of model membranes composed of phosphatidylcholines containing linear saturated fatty acyl chains. Biochemistry. 1987;26:6118–26.
[82] Hernandez-Borrell J, Keough KMW. Heteroacid phosphatidylcholines with different amounts of unsaturation respond differently to cholesterol. Biochimica et Biophysica Acta (BBA) - Biomembranes. 1993;1153:277-82.
[83] Ulrich AS, Sami M, Watts A. Hydration of DOPC bilayers by differential scanning calorimetry. Biochimica et Biophysica Acta (BBA) - Biomembranes. 1994;1191:225-30.
[84] Keough KMW. Modifications of lipid structure and their influence on mesomorphism in model membranes: the influence of hydrocarbon chains. Biochemistry and Cell Biology. 1986;64:44-9.
[85] New RRC. Liposomes : a practical approach. Oxford ; New York: Oxford University Press; 1990.
[86] Graham Shipley G, Green JP, Nichols BW. The phase behavior of monogalactosyl, digalactosyl, and sulphoquinovosyl diglycerides. Biochimica et Biophysica Acta (BBA) - Biomembranes. 1973;311:531-44.
[87] Silvius JR. Thermotropic Phase Transitions of Pure Lipids in Model Membranes and Their Modifications by Membrane Proteins. New York: John Wiley & Sons; 1982.
[88] Bach D, Miller IR. Glyceryl monooleate black lipid membranes obtained from squalene solutions. Biophysical Journal. 1980;29:183-7.
[89] Hladky SB, Gruen DW. Thickness fluctuations in black lipid membranes. Biophysical Journal. 1982;38:251-8.
[90] Miller IR. Energetics of fluctuation in lipid bilayer thickness. Biophysical Journal. 1984;45:643-4.
[91] Jacob N. Israelachvili, Wennerstroem H. Entropic forces between amphiphilic surfaces in liquids. The Journal of Physical Chemistry 1992;96:520–31.
[92] Movileanu L, Popescu D, Ion S, Popescu AI. Transbilayer Pores Induced by Thickness Fluctuations. Bulletin of Mathematical Biology. 2006;68:1231-55.
[93] Bennett WF, Sapay N, Tieleman DP. Atomistic simulations of pore formation and closure in lipid bilayers. Biophys J. 2014;106:210-9.
[94] Orsia M, Essex JW. Permeability of drugs and hormones through a lipid bilayer: insights from dual-resolution molecular dynamics. Soft Matter. 2010;6:3797–808.
[95] Henzler-Wildman K, Kern D. Dynamic personalities of proteins. Nature. 2007;450:964-72.
[96] Farago B, Monkenbusch M, Goecking KD, Richter D, Huang JS. Dynamics of Microemulsions as Seen by Neutron Spin-Echo. Physica B-Condensed Matter. 1995;213:712-7.
[97] Nagao M. Observation of local thickness fluctuations in surfactant membranes using neutron spin echo. Phys Rev E Stat Nonlin Soft Matter Phys. 2009;80:031606.
[98] Lee V, Hawa T. Investigation of the effect of bilayer membrane structures and fluctuation amplitudes on SANS/SAXS profile for short membrane wavelength. J Chem Phys. 2013;139:124905.
[99] Bingham RJ, Smye SW, Olmsted PD. Dynamics of an asymmetric bilayer lipid membrane in a viscous solvent. Europhysics Letters (EPL). 2015;111:18004.

[100] Flenner E, Das J, Rheinstadter MC, Kosztin I. Subdiffusion and lateral diffusion coefficient of lipid atoms and molecules in phospholipid bilayers. Phys Rev E Stat Nonlin Soft Matter Phys. 2009;79:011907.
[101] Akimoto T, Yamamoto E, Yasuoka K, Hirano Y, Yasui M. Non-Gaussian fluctuations resulting from power-law trapping in a lipid bilayer. Phys Rev Lett. 2011;107:178103.
[102] Falck E, Rog T, Karttunen M, Vattulainen I. Lateral diffusion in lipid membranes through collective flows. J Am Chem Soc. 2008;130:44-5.
[103] Sharma VK, Mamontov E, Tyagi M, Qian S, Rai DK, Urban VS. Dynamical and Phase Behavior of a Phospholipid Membrane Altered by an Antimicrobial Peptide at Low Concentration. J Phys Chem Lett. 2016;7:2394-401.
[104] Sharma VK, Mamontov E, Anunciado DB, O'Neill H, Urban VS. Effect of antimicrobial peptide on the dynamics of phosphocholine membrane: role of cholesterol and physical state of bilayer. Soft Matter. 2015;11:6755-67.
[105] Gupta S, De Mel JU, Perera RM, Zolnierczuk P, Bleuel M, Faraone A, et al. Dynamics of Phospholipid Membranes beyond Thermal Undulations. The Journal of Physical Chemistry Letters. 2018;9:2956-60.
[106] Gerstl C, Schneider GJ, Fuxman A, Zamponi M, Frick B, Seydel T, et al. Quasielastic Neutron Scattering Study on the Dynamics of Poly(alkylene oxide)s. Macromolecules. 2012;45:4394-405.
[107] Schneider GJ, Nusser K, Neueder S, Brodeck M, Willner L, Farago B, et al. Anomalous chain diffusion in unentangled model polymer nanocomposites. Soft Matter. 2013;9:4336.
[108] Pincet F, Adrien V, Yang R, Delacotte J, Rothman JE, Urbach W, et al. FRAP to Characterize Molecular Diffusion and Interaction in Various Membrane Environments. PloS one. 2016;11:e0158457-e.
[109] Johnson ME, Berk DA, Blankschtein D, Golan DE, Jain RK, Langer RS. Lateral diffusion of small compounds in human stratum corneum and model lipid bilayer systems. Biophysical Journal. 1996;71:2656-68.
[110] Gaede HC, Gawrisch K. Lateral Diffusion Rates of Lipid, Water, and a Hydrophobic Drug in a Multilamellar Liposome. Biophysical Journal. 2003;85:1734-40.
[111] Busch S, Unruh T. The influence of additives on the nanoscopic dynamics of the phospholipid dimyristoylphosphatidylcholine. Biochim Biophys Acta. 2011;1808:199-208.
[112] Kuśba J, Li L, Gryczynski I, Piszczek G, Johnson M, Lakowicz JR. Lateral Diffusion Coefficients in Membranes Measured by Resonance Energy Transfer and a New Algorithm for Diffusion in Two Dimensions. Biophysical Journal. 2002;82:1358-72.
[113] Kawaguchi T, Kita R, Shinyashiki N, Yagihara S, Fukuzaki M. The Bi-modality Diffusion of Water Molecules in Liposome/Water Dispersion Systems Analyzed by Pulsed Field Gradient Spin Echo NMR Method. Transactions of the Materials Research Society of Japan. 2016;41:359-62.
[114] Moore PB, Lopez CF, Klein ML. Dynamical Properties of a Hydrated Lipid Bilayer from a Multinanosecond Molecular Dynamics Simulation. Biophysical Journal. 2001;81:2484-94.
[115] Roberts MF, Redfield AG. High-Resolution 31P Field Cycling NMR as a Probe of Phospholipid Dynamics. Journal of the American Chemical Society. 2004;126:13765-77.
[116] Essmann U, Berkowitz ML. Dynamical Properties of Phospholipid Bilayers from Computer Simulation. Biophysical Journal. 1999;76:2081-9.

[117] Klauda JB, Roberts MF, Redfield AG, Brooks BR, Pastor RW. Rotation of Lipids in Membranes: Molecular Dynamics Simulation, 31P Spin-Lattice Relaxation, and Rigid-Body Dynamics. Biophysical Journal. 2008;94:3074-83.
[118] Contreras FX, Sánchez-Magraner L, Alonso A, Goñi FM. Transbilayer (flip-flop) lipid motion and lipid scrambling in membranes. FEBS Letters. 2010;584:1779-86.
[119] Devaux PF, Herrmann A, Ohlwein N, Kozlov MM. How lipid flippases can modulate membrane structure. Biochimica et Biophysica Acta (BBA) - Biomembranes. 2008;1778:1591-600.
[120] McConnell HM, Kornberg RD. Inside-outside transitions of phospholipids in vesicle membranes. Biochemistry. 1971;10:1111-20.
[121] Pantaler E, Kamp D, Haest CWM. Acceleration of phospholipid flip-flop in the erythrocyte membrane by detergents differing in polar head group and alkyl chain length. Biochimica et Biophysica Acta (BBA) - Biomembranes. 2000;1509:397-408.
[122] Allhusen JS, Conboy JC. The Ins and Outs of Lipid Flip-Flop. Accounts of Chemical Research. 2017;50:58-65.
[123] Marquardt D, Heberle FA, Miti T, Eicher B, London E, Katsaras J, et al. (1)H NMR Shows Slow Phospholipid Flip-Flop in Gel and Fluid Bilayers. Langmuir : the ACS journal of surfaces and colloids. 2017;33:3731-41.
[124] Inokuchi T, Arai N. Relationship between water permeation and flip-flop motion in a bilayer membrane. Physical Chemistry Chemical Physics. 2018;20:28155-61.
[125] Ogushi F, Ishitsuka R, Kobayashi T, Sugita Y. Flip-Flop Motions of Lipid Molecules in Mixed Bilayer Systems. Biophysical Journal. 2010;98:489a.
[126] Sapay N, Bennett WFD, Tieleman DP. Molecular Simulations of Lipid Flip-Flop in the Presence of Model Transmembrane Helices. Biochemistry. 2010;49:7665-73.
[127] Choubey A, Kalia RK, Malmstadt N, Nakano A, Vashishta P. Cholesterol translocation in a phospholipid membrane. Biophysical journal. 2013;104:2429-36.
[128] Nakano M, Fukuda M, Kudo T, Matsuzaki N, Azuma T, Sekine K, et al. Flip-Flop of Phospholipids in Vesicles: Kinetic Analysis with Time-Resolved Small-Angle Neutron Scattering. The Journal of Physical Chemistry B. 2009;113:6745-8.
[129] Nguyen MHL, DiPasquale M, Rickeard BW, Stanley CB, Kelley EG, Marquardt D. Methanol Accelerates DMPC Flip-Flop and Transfer: A SANS Study on Lipid Dynamics. Biophysical Journal. 2019.